Dynamics and chaos in the unified scalar field cosmology. II. System in a finite box

Giovanni Acquaviva[*] and Georgios Lukes-Gerakopoulos[†]

Institute of Theoretical Physics, Faculty of Mathematics and Physics, Charles University in Prague, 18000 Prague, Czech Republic

We revisit the global dynamics of unified dark matter cosmological models and analyze it in a new dynamical system setting. In particular, by defining a suitable set of variables we obtain a bounded variable space, a feature that allows a better control of the critical elements of the system. First, we give a comprehensive cosmological interpretation of the critical points. Then, we turn our focus on particular representative trajectories with physically motivated initial conditions studied in the first paper of the series, and we discuss how the scale factor relates to the equation of state parameter. We review and complement these results in the light of the new variable approach by discussing the issue of whether the system is chaotic or not.

I. INTRODUCTION

The current standard cosmological model is the Λ cold dark matter (ΛCDM) scenario, which includes two elements whose components have unknown nature: the dark matter and the dark energy. This simple model fits quite well the observed behavior of our Universe [1,2] at least from the matter-dominated epoch on, where structure formation starts. However, the nature of both the dark components is still elusive and it is matter of intense debate; see, e.g., [3,4] for a broad overview. While part of the literature approaches the study of this topic by keeping the dark sector divided into two separate components, efforts have been put also into unifying the effect of both dark energy and dark matter under the same mechanism, for example through the modified Chaplygin gas models (see, e.g., [5] and references therein). Along the same lines, in [6,7] a scalar field potential was introduced, which is able to act both as dark matter and dark energy, hence dubbed unified dark matter (UDM). Since its introduction it has been the subject of detailed analysis [8–13].

Here we revisit the dynamical aspect of the UDM cosmology first addressed in [8], where such a scalar field was studied in the background of a spatially curved Friedmann-Robertson-Walker (FRW) spacetime. The resulting cosmological model was recast as a Hamiltonian system of two coupled oscillators and studied as such. The phase space of the system was unbounded and allowed trajectories to escape to infinity. Moreover, in the case of a positive spatial curvature, indications of chaotic behavior were found for some sets of initial conditions. These indications were based on transient features of the characteristic Lyapunov number and of a similar chaotic indicator, so the chaotic behavior was called chaotic scattering instead of chaos. In general, when

one addresses the issue of whether a dynamical system suffering escapes exhibits chaos or not, Lyapunov-like indicators should be used with caution; see, e.g., [14]. In fact, in the literature there is a variety of approaches different from Lyapunov-like indicators to address the search for chaos in scalar field cosmologies, starting, e.g., from Page [15] to more recent developments such as [16,17] and references therein.

In the present paper we mainly address the study of the same cosmological model as in [8], but we introduce a different parametrization of the dynamical variables. This parametrization confines the system "in a box," i.e. in a bounded variable space. Such reparametrization has been widely used in previous works on cosmological dynamical systems (see, e.g., [18–22]) and it is especially useful in treating cosmological models with spatial positive curvature, where the possibility of recollapsing universes has to be taken into account. In fact, in such models, the usual definition of *expansion-normalized variables* is doomed to present singular behavior in the turning points of the scale factor.

Such reparametrization allows us to uncover new information regarding the dynamics of the system. On one hand it allows us to study the specific features of the cosmological model encoded in the critical points. On the other hand it allows us to have a new perspective on the dynamics of the system. Namely, in the box version of the UDM model we have sinks, and every orbit will end up in one of these sinks. Thus, by studying the structure of the basins of attraction of these sinks we can tell whether the system is chaotic or not. If a system is chaotic, then the sensitivity on the initial condition will be represented by a fractal structure of the basins of attraction; see, e.g., [23,24], and references therein. Our analysis shows that the basins of attraction do not have a fractal structure, so the orbital dynamics of the UDM model should not be chaotic, which is in fact in agreement with [16].

[*]gioacqua@utf.troja.mff.cuni.cz
[†]gglukes@gmail.com

043525-1

The paper is structured as follows. In Sec. II we present and analyze the UDM cosmological model. We first briefly review the Hamiltonian formulation and then provide the bounded dynamical system; the latter is analyzed in detail from both mathematical and cosmological perspectives. In Sec. III we focus on the analysis of some representative orbits of the variable space, providing their interpretation in cosmological terms; moreover, we address the problem of the lack of chaos in the system by inspecting the basins of attraction of the sinks. Eventually, Sec. IV summarizes the main results. In this work the geometric units are employed.

II. THEORETICAL ANALYSIS

A. The cosmological model

We consider a cosmological model described by the homogeneous and isotropic FRW metric,

$$ds^2 = -dt^2 + a^2(t)\left[\frac{dr^2}{1-kr^2} + r^2 d\theta^2 + r^2\sin^2\theta d\phi^2\right], \quad (1)$$

where a is the scale factor. Open, flat and closed spatial geometries correspond respectively to $k < 0$, $k = 0$ and $k > 0$. In the following we will be interested in the spatially closed case, which allows for recollapsing cosmological scenarios. As a source in Einstein's field equations we consider the energy-momentum tensor $T^{\mu\nu}$ of a massive scalar field, uniquely described by its energy density and its pressure given respectively by

$$\rho_\phi = -T_0^0 = \frac{1}{2}\dot{\phi}^2 + U(\phi), \quad (2)$$

$$p_\phi = T_j^i = \frac{1}{2}\dot{\phi}^2 - U(\phi), \quad (3)$$

where the $\cdot$ symbol indicates the derivative with respect to the cosmic time t. Hereafter, we assume an effective barotropic equation of state (EoS) $p_\phi = w\rho_\phi$ for the scalar field. The potential U in [7,8] was chosen to have the form

$$U(\phi) = c_1\cosh^2\left(\sqrt{\frac{3}{8}}\phi\right) + c_2, \quad (4)$$

where c_1 and c_2 are real constants. In order for the field to have a real non-negative mass, such constants are required to satisfy the conditions $c_1 \geq 0$ and $c_1 + c_2 \geq 0$ [7,8]. As already stated before, this kind of scalar fluid has been considered as a possible candidate for unifying the effect of the whole dark sector.

An alternative form of the potential [12] reads

$$U(\phi) = b_1\left(1 + 3\cosh^2\left(\sqrt{\frac{3}{8}}\phi\right)\right)$$
$$+ b_2\left(3\cosh\left(\sqrt{\frac{3}{8}}\phi\right) + \cosh^3\left(\sqrt{\frac{3}{8}}\phi\right)\right). \quad (5)$$

In the Appendix we discuss briefly the case $b_1 = b_2$, i.e.

$$U(\phi) = b_1\left(1 + \cosh\left(\sqrt{\frac{3}{8}}\phi\right)\right)^3, \quad (6)$$

which is a particular case of a potential already introduced in [6].

By implementing metric (1) and source (2), (3) into Einstein's field equations and explicating the covariant conservation of energy-momentum, the following system is obtained:

$$H^2 + \frac{k}{a^2} = \frac{1}{6}\dot{\phi}^2 + \frac{1}{3}U(\phi), \quad (7)$$

$$2\dot{H} + 3H^2 + \frac{k}{a^2} = -\frac{1}{2}\dot{\phi}^2 + U(\phi), \quad (8)$$

$$\ddot{\phi} + 3H\dot{\phi} + \partial_\phi U = 0, \quad (9)$$

where we employed the Hubble expansion parameter $H = \dot{a}/a$.

B. UDM as coupled oscillators

In [8] the UDM cosmology was expressed in terms of two coupled oscillators. To achieve that the variables were changed from (a, ϕ) to

$$x = Aa^{3/2}\sinh(c\phi)$$
$$y = Aa^{3/2}\cosh(c\phi) \quad (10)$$

with $c^2 = 3/8$. This transformation results in a Hamiltonian function

$$\mathcal{H} = \frac{1}{2}\left[\left(p_x^2 - \frac{3}{4}c_2 x^2\right) - \left(p_y^2 - \frac{3}{4}(c_1 + c_2)y^2\right)\right]$$
$$- \frac{1}{2}[3^{4/3}k(y^2 - x^2)^{1/3}] \quad (11)$$

where $p_x = \dot{x}$, $p_y = -\dot{y}$ denote the canonical momenta. The Hamiltonian function (11) describes two coupled oscillators, which makes the UDM analysis more dynamically intuitive. However, since $c_1 + c_2 \geq 0$, the constant c_2 can be negative and one of the oscillators offers hyperbolic solutions; this implies the presence of trajectories escaping to infinity $(a \to \infty)$ even if $k > 0$. Moreover, a closed universe implies

also the possibility of recollapsing models ($a \to 0$). Since in this coupled oscillators formalism the system suffers from escapes to infinity and recollapses, the phase space is not bounded (see [13] for details), and this brings along certain difficulties in performing a dynamical study of the UDM cosmology [8]. In the following section we overcome the unboundedness by performing a novel reparametrization.

C. UDM in a box

In constructing a cosmological dynamical system with flat or negative curvature, it is usually sufficient to define dimensionless variables by normalizing the relevant dynamical quantities over the expansion H. However, as we are considering geometries with $k > 0$, such a choice includes recollapsing solutions. While cosmological observations [1] tend to rule out the presence of a nonvanishing spatial curvature, we are especially interested in including in the picture the possibility of recollapse because of its rich and interesting dynamics [25]. However, a recollapsing scenario can lead to singular behaviors of the usual normalized variables in the turning points of the scale factor, where $H = 0$. This problem can be circumvented by noting that, while H alone can vanish during the evolution, the left-hand side of Eq. (7) instead is always positive. Hence, one can define a new set of variables by normalizing over the quantity

$$D = \sqrt{H^2 + \frac{k}{a^2}}.$$ (12)

The dimensionless variables obtained with such choice are the following:

$$X_\phi = \frac{\dot\phi}{\sqrt{6}D},$$ (13)

$$X_U = \frac{\sqrt{U}}{\sqrt{3}D},$$ (14)

$$X_H = \frac{H}{D},$$ (15)

$$X_{\partial U} = -\frac{\partial_\phi U}{U},$$ (16)

$$F = \frac{\partial_\phi^2 U}{U}.$$ (17)

The definitions (16) and (17) are inspired by the quantities used in the study of cosmological tracking solutions (see, e.g., [26,27]). The function F has to be included in order to close the system, but we stress the fact that it does not act as an independent variable. In fact, knowing in principle the dependence of the potential on the field, one could invert Eq. (16) and obtain $\phi = \phi(X_{\partial U})$, which could then be

plugged into Eq. (17) to obtain $F(X_{\partial U})$. In the specific case of potential (4), one can see that the function $X_{\partial U}$ is invertible in the whole range of ϕ only if $\alpha = c_2/c_1 \geq -1/2$; however, if $-1 < \alpha < -1/2$ the inversion can be carried out only piecewise because the function is not monotonic anymore. Here, we focus our attention on the range $\alpha \geq -1/2$ which, apart from including physically relevant situations, allows for a quite general description, as the features of the critical elements of the variable space turn out to be effectively independent of the specific value of α. Hence, if $\alpha \geq -1/2$, the function $X_{\partial U}$ is monotonic in ϕ and bounded. It is then straightforward to find ϕ as function of $X_{\partial U}$, i.e.

$$\phi = \sqrt{\frac{2}{3}}\log\left[\frac{\sqrt{1 + \frac{8}{3}X_{\partial U}^2\alpha(1 + \alpha)} - \sqrt{\frac{2}{3}}X_{\partial U}(1 + 2\alpha)}{1 + \sqrt{\frac{2}{3}}X_{\partial U}}\right]$$ (18)

as a consequence of the boundedness of $X_{\partial U}$, which is defined in the range $X_{\partial U} \in [-\sqrt{3/2}, \sqrt{3/2}]$. Expression (18) can be plugged into Eq. (17) in order to express it as a function of $X_{\partial U}$, that is

$$F(X_{\partial U}) = \frac{(1 + 2\alpha)\sqrt{1 + \frac{8}{3}\alpha(1 + \alpha)X_{\partial U}^2} - 1}{\frac{8}{3}\alpha(1 + \alpha)}.$$ (19)

With regard to other variables (13)–(15), it is easy to check that they are bounded as well. First of all, by recasting Eq. (7) in terms of the normalized variables one obtains

$$X_\phi^2 + X_U^2 = 1.$$ (20)

Given that $X_U \geq 0$, then $X_\phi \in [-1, 1]$ and $X_U \in [0, 1]$. Finally, the variable X_H is clearly defined in the interval $[-1, 1]$; moreover, we notice that this variable is positive/negative iff the Universe is expanding/collapsing.

In order to build the dynamical system, it will be useful to write both Eq. (8) and the evolution equation of the quantity D in terms of the new variables

$$\frac{\dot H}{D^2} = \frac{3}{2}(X_U^2 - X_\phi^2) - X_H^2 - \frac{1}{2},$$ (21)

$$\frac{\dot D}{D^2} = \frac{3}{2}X_H(X_U^2 - X_\phi^2 - 1).$$ (22)

Defining the new "time" derivative $X' = D^{-1}\dot X$, the autonomous dynamical system is constructed by taking the prime derivative of the normalized variables (13)–(16). Then, by implementing Eq. (9) and Eqs. (20)–(22), the system takes the following form:

$$X_\phi' = \sqrt{\frac{3}{2}}(1 - X_\phi^2)(X_{\partial U} - \sqrt{6}X_H X_\phi), \qquad (23)$$

$$X_H' = (1 - X_H^2)(1 - 3X_\phi^2), \qquad (24)$$

$$X_{\partial U}' = -\sqrt{6}X_\phi(F - X_{\partial U}^2), \qquad (25)$$

where F is the function of $X_{\partial U}$ previously defined, which in terms of the parameters of the potential reads

$$F = \frac{(c_1 + 2c_2)\sqrt{c_1^2 + \frac{8}{3}c_2(c_1 + c_2)X_{\partial U}^2} - c_1^2}{\frac{8}{3}c_2(c_1 + c_2)}. \qquad (26)$$

By building the system in this way we decouple the evolution of D from the rest of the variables and, through the constraint (20), we can disregard the evolution of X_U. Note that the quantities $X_{\partial U}^2$ and F are known in cosmology as the "slow-roll parameters," ϵ and $|\eta|$ respectively; this means that an exponential behavior of the scale factor is an expected feature whenever $|X_{\partial U}| \ll 1$ [28].

The scale factor as a function of the new variables is

$$a = \frac{\sqrt{3k}X_U}{\sqrt{1 - X_H^2}\sqrt{c_1 \cosh^2(\sqrt{\frac{3}{8}}\phi) + c_2}}, \qquad (27)$$

where ϕ is given by Eq. (18).

D. Analysis and interpretation of critical points

The critical points of the system are those values of the variables $\{X_\phi, X_H, X_{\partial U}\}$ for which $\mathbf{X}' = 0$ is satisfied. The stability of critical points is then analyzed by inspecting the eigenvalues of the Jacobian matrix evaluated at the points themselves. If the real part of all the eigenvalues is negative (positive) then the critical point is a sink (a source), while if the sign of the eigenvalues is mixed then the critical point is a saddle; in the latter case, the stable eigendirections are given by the eigenvectors corresponding to the negative eigenvalues. For the system (23)–(25) we list the critical points, their stability and cosmological interpretation in Table I, while their location inside the invariant subsets are shown in Figs. 1–3 for the specific choice $\alpha = 1$. In such plots we specify with dots the locations of sources (blue), sinks (green) and saddles (black). It is worth noting that both the location and the stability of the critical points are independent of the values of the parameters c_1 and c_2 as long as their ratio $\alpha \geq -1/2$, so that the situations portrayed are easily generalizable. Here we discuss in detail the cosmological interpretation of the critical points. This can be done by calculating the deceleration parameter q and the effective EoS parameter w, which are given respectively by

TABLE I. Critical points of the system, their stability and corresponding cosmological parameters.

$\{X_\phi, X_H, X_{\partial U}\}$	Stability	q	w
$\{0, -1, 0\}$	Source	-1	-1
$\{0, 1, 0\}$	Sink	-1	-1
$\{\pm 1, 1, \pm\sqrt{3/2}\}$	Source	2	1
$\{\pm 1, -1, \mp\sqrt{3/2}\}$	Sink	2	1
$\{\pm 1, 1, \mp\sqrt{3/2}\}$	Saddle	2	1
$\{\pm 1, -1, \pm\sqrt{3/2}\}$	Saddle	2	1
$\{\pm 1/2, 1, \pm\sqrt{3/2}\}$	Saddle	$-1/4$	$-1/2$
$\{\pm 1/2, -1, \mp\sqrt{3/2}\}$	Saddle	$-1/4$	$-1/2$
$\{\pm 1/\sqrt{3}, \pm\sqrt{3/2}, \sqrt{3/2}\}$	Saddle	0	$-1/3$
$\{\pm 1/\sqrt{3}, \mp\sqrt{3/2}, -\sqrt{3/2}\}$	Saddle	0	$-1/3$

$$q = \frac{3X_\phi^2 - 1}{X_H^2}, \qquad (28)$$

$$w = 2X_\phi^2 - 1. \qquad (29)$$

Eventually, one can calculate the cosmic time-dependent scale factor of the models by integrating Eqs. (21), (22) in the critical points.
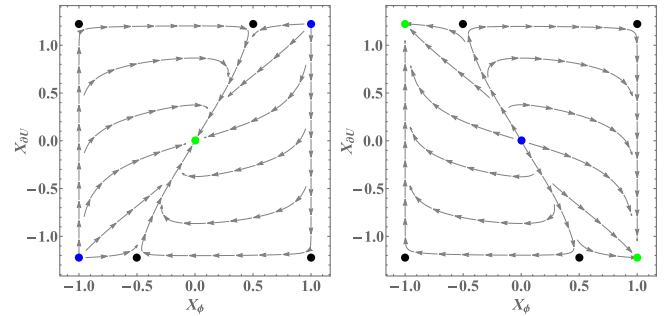

FIG. 1. Invariant sets $X_H = 1$ (left panel) and $X_H = -1$ (right panel). The points identify sources (blue), saddles (black) and sinks (green).
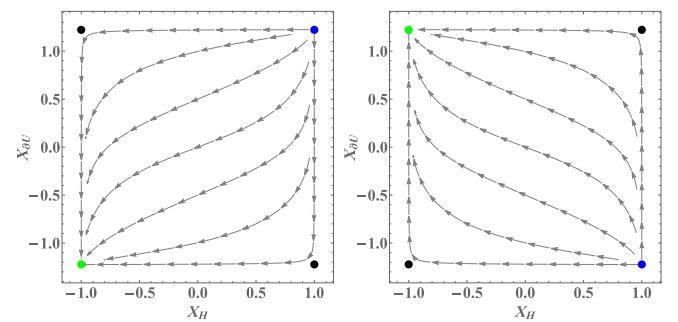

FIG. 2. Invariant sets $X_\phi = 1$ (left panel) and $X_\phi = -1$ (right panel). The points identify sources (blue), saddles (black) and sinks (green).
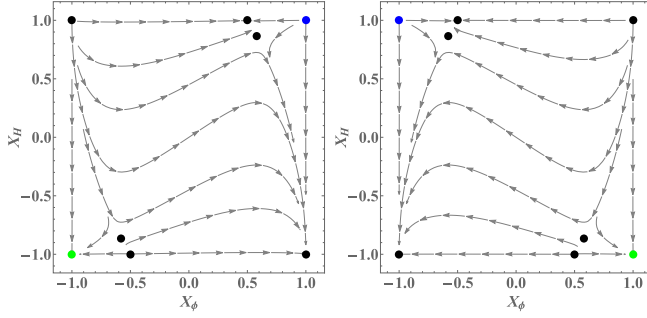
FIG. 3. Invariant sets $X_{\partial U} = \sqrt{3/2}$ (left panel) and $X_{\partial U} = -\sqrt{3/2}$ (right panel). The points identify sources (blue), saddles (black) and sinks (green).

There are three sources in the variable space. The point $\{0, -1, 0\}$ is located in the invariant subset $X_H = -1$ and hence describes collapsing models with negligible curvature with respect to the Hubble parameter. Moreover, the fact that $X_\phi = 0$ implies that the field's potential energy dominates over the kinetic energy; hence, these models are collapsing exponentially, i.e. $a \sim e^{-H_0 t}$, starting from the infinite past of cosmic time. As expected, the parameters q and w have the values corresponding to a cosmological constant. The other two sources $\{\pm 1, 1, \pm\sqrt{3/2}\}$ instead, being in the invariant set $X_H = 1$, describe expanding models with negligible curvature. In these points the kinetic energy dominates and the cosmological parameters are $q = 2$ and $w = 1$, corresponding to a stiff matter behavior. The scale factor is polynomial: in fact, both points describe models with $a \sim t^{1/3}$ in the phase near the big bang $a \to 0$.

There are also three sinks and for their interpretation one follows the same approach as for the previous ones. The point $\{0, 1, 0\}$, in the invariant subset $X_H = 1$, is an asymptotically expanding model with exponential scale factor $a \sim e^{H_0 t}$ and parameters $q = w = -1$. The other two sinks $\{\pm 1, -1, \mp\sqrt{3/2}\}$ represent polynomially collapsing models with $a \sim t^{-1/3}$ and stiff matter behavior. All these points describe phases with negligible curvature.

Finally, the variable space has a number of saddle points which act as transients for some trajectories. The points $\{\pm 1/2, 1, \pm\sqrt{3/2}\}$ describe expanding flat models with scale factor $a \sim t^{4/3}$, while at points $\{\pm 1/2, -1, \mp\sqrt{3/2}\}$ the models are collapsing with scale factor $a \sim t^{-4/3}$. For both pairs of points we have $w = -1/2$, which is a common EoS parameter found in quintessence models. The points $\{\pm 1/\sqrt{3}, \sqrt{3}/2, \pm\sqrt{3/2}\}$ present a different behavior from the other cases, because the curvature here is not negligible with respect to the expansion: in this case the model is linearly expanding with $a \sim t$ and the EoS parameter $w = -1/3$ is the one corresponding to a "curvature fluid." The same goes for the points $\{\pm 1/\sqrt{3}, -\sqrt{3}/2, \mp\sqrt{3/2}\}$, with the difference that these describe collapsing phases with $a \sim t^{-1}$.

One should note that the system defined by the Hamiltonian of Secs. II A and II B is conservative, in the sense that Liouville's theorem ensures preservation of the phase-space volumes under the Hamiltonian flow. Or, equivalently, there are no attractors in the Hamiltonian system when the trajectories are plotted in canonical coordinates. We stress this since it has been shown that apparent attractors can appear when Lagrangian variables are used instead of the canonical ones [29]. However, it is a quite well-known procedure to transform a nonconservative system into a conservative one and vice versa by combining variables and evolution parameter transformations [30], which is actually what was performed in Sec. II C.

III. ORBITAL ANALYSIS

The critical points tell us about the basic global structure of the model, but they do not tell us all the details of how individual initial conditions evolve. To study individual evolutions is like doing orbital analysis of the system. In [8] the dynamical study was reduced to the case $c_1 = c_2 = 1$ with $k = 10^{-3}$ which was called the "semiflat" model, and in particular the following five initial conditions were considered: (1) $y = 0.0001$, $x = 0$, $p_x = 0.006$; (2) $y = 0.0001$, $x = 0$, $p_x = 0.03$; (3) $y = 0.0001$, $x = 0$, $p_x = 0.04$; (4) $y = 0.0001$, $x = 0$, $p_x = 0.041$; (5) $y = 0.0001$, $x = 0$, $p_x = 0.099$, where the missing variable p_y was evaluated through Eq. (11) with $\mathcal{H} = 0$ and by choosing the negative sign in front of the square root of p_y^2.

The analysis in Sec. II D showed us that the structure of the parameter space of UDM cosmology is independent of α in the range $\alpha \geq -\frac{1}{2}$, i.e. for any pair of c_1, c_2 satisfying such condition the nature of the critical points does not change. Thus, for simplicity and without loss of generality one can indeed choose $c_1 = c_2 = 1$ to study the dynamics.

In the top panel of Fig. 4 we show the five representative trajectories evolving inside the three-dimensional variable space. We implement the same initial conditions by translating them to the variables $\{X_\phi, X_H, X_{\partial U}\}$, through the following transformation formulas:

$$X_\phi = \frac{y\dot{x} - x\dot{y}}{\sqrt{3^{4/3}k(y^2 - x^2)^{4/3} + (y\dot{y} - x\dot{x})^2}}, \tag{30}$$

$$X_H = \frac{y\dot{y} - x\dot{x}}{\sqrt{3^{4/3}k(y^2 - x^2)^{4/3} + (y\dot{y} - x\dot{x})^2}}, \tag{31}$$

$$X_{\partial U} = \sqrt{\frac{3}{2}} \frac{c_1 xy}{(c_1 + c_2)y^2 - c_2 x^2}. \tag{32}$$

Orbit 1 ends in the sink $\left\{1, -1, -\sqrt{\frac{3}{2}}\right\}$ following approximately the flow of the invariant set shown in the top panel of Fig. 2. Orbits 2 and 3 end up in the sink $\left\{-1, -1, \sqrt{\frac{3}{2}}\right\}$.
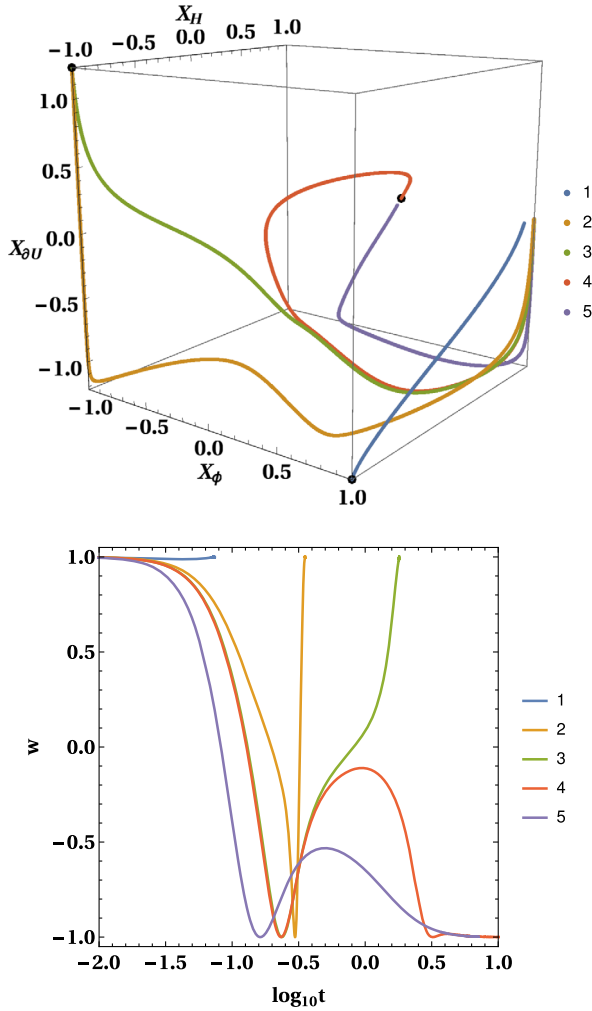
FIG. 4. Top panel: Five representative trajectories in the variable space; the initial conditions corresponding to the numbers are given in the text; the dots indicate the attractors. Bottom panel: The evolution of the effective EoS parameter as a function of the cosmic time for the same initial conditions.

These different recollapsing scenarios could not be discerned in the Hamiltonian formalism. Orbits 4 and 5 end up in the de Sitter sink $\{0, 1, 0\}$. Moreover, we know now from a dynamical point of view why orbits 3 and 4 split from each other after evolving almost identically for a considerable time. Namely, orbits 3 and 4 follow the flow along the separatrix on the invariant set shown in the right panel of Fig. 3, until they reach the saddle point $\left(-\frac{1}{\sqrt{3}}, \frac{\sqrt{3}}{2}, -\sqrt{\frac{3}{2}}\right)$ where they split following two different eigendirections. The evolution of the EoS parameter for all these orbits as a function of the cosmic time is shown in the bottom panel of Fig. 4. Apparently all the initial conditions correspond to an initial epoch where stiff matter EoS $w = 1$ dominates. Orbit 1 does not deviate much from this behavior and quite soon enters the recollapsing phase. All the other orbits passing through all the intermediate values of w reach a transitory phase of exponential

expansion ($w = -1$). After this common de Sitter phase, orbits 2 and 3 return to a stiff-matter phase by following a recollapsing dynamics. For orbit 4 instead the EoS parameter momentarily increases up to a dustlike behavior $w = 0$, before returning to the de Sitter expansion with $w = -1$. As for orbit 5, its final fate is the same as trajectory 4 but the intermediate phase reaches $w = -1/2$.

A. Remarks on the equation of state

The evolution of the scale factor of orbits 4 and 5 should be qualitatively close to the ΛCDM model [8]. However, by comparing Fig. 1(b) of [8] with the bottom panel of Fig. 4, we can see that the EoS parameter values are not in complete agreement with the inclinations of the scale factor's logarithmic plot. For example the scale factor of orbit 4 appears to follow the matter-dominated era inclination, i.e. $a \propto t^{2/3}$, at $-0.6 \lesssim \log_{10} t \lesssim 0$, but for this time range w undergoes a transition from -1 to 0 and back to -1. Thus, the following two questions arise: (a) Are the UDM models compatible with an effective description using a barotropic equation of state? (b) Can one infer the dominating era of a component of the Universe by the evolution of the scale factor?

To answer these questions we searched for a trajectory having $w \approx 0$ for a considerable time. Since we want to impose $w = 0$, from Eq. (29) we get that this is achieved when $X_\phi^2 = 1/2$. Moreover, we want the scenario to be expanding and the curvature to be negligible in comparison to the expansion, so $X_H \approx 1$. In order to find the appropriate value for $X_{\partial U}$ we performed a scan in the range of its possible values, i.e. $[-\sqrt{3/2}, \sqrt{3/2}]$, and Fig. 5 shows the scenario which we were looking for. Namely, the parameter w (continuous curve) behaves like dust from the start until $t \approx 1$, with negligible variations; in this time range, since the fluid is barotropic, one would anticipate that the scale factor should grow approximately like $a \propto t^{2/3}$ since the scale factor for a barotropic fluid grows like
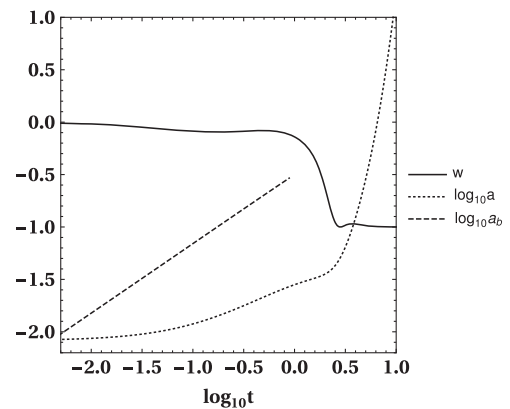

FIG. 5. The scale factor a and the EoS parameter w as functions of the cosmic time t for a trajectory starting from $(-1/\sqrt{2}, 0.8, -\sqrt{3/2} + 0.03)$. a_b shows the evolution of the scale factor in the matter-dominated era, if we assume constant w.
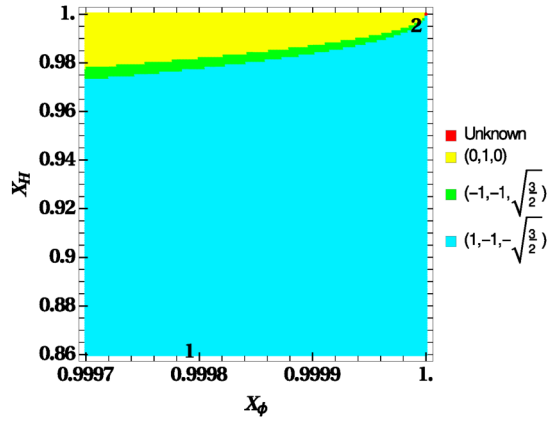
FIG. 6. A portion of the plane $X_{\partial U} = 0$. The numbers 1 and 2 identify the initial conditions for the respective trajectories of Fig. 4. The colors correspond to the basins of attraction of the three sinks for the points in the plane.

$$a_b \propto t^{\frac{2}{3(1+w)}}, \qquad (33)$$

when w is almost constant. The dashed line shows a_b when w is given by Eq. (29), with the initial value of a_b appropriately rescaled in order to fit the initial value of the dotted line. The dotted line, in turn, shows the evolution of the scale factor a as it comes from the equations of motion (23)–(25) when the inversion equation (27) is applied; note that in the latter case no assumption is made regarding the EoS. We see that the dashed and the dotted curves do not match, so one would assume that the scalar field is not behaving like a barotropic fluid in the matter-dominated era. However, such conclusion would be wrong. If one wants to do the check properly, then from the stress-energy conservation, i.e.

$$\dot{\rho}_\phi + 3H(\rho_\phi + p_\phi) = 0, \qquad (34)$$

one gets, by assuming a barotropic fluid behavior for the scalar field, that

$$\rho_\phi(a) = \rho_\phi(a_0) \exp\left(-\int_a^{a_0} \frac{3(1+w(\tilde{a}))}{\tilde{a}} d\tilde{a}\right). \qquad (35)$$

Equation (35) is then substituted into Eq. (7). The solution of the resulting equation after the above substitution is giving the scale factor with respect to the cosmic time. Note that we take the positive root of $\dot{a}$, since we anticipate an expanding universe. By following the above procedure in which we employ the numerical found data one gets a scale factor evolution which reproduces the dotted line of Fig. 5. Thus, (a) the UDM scalar field is behaving like a barotropic fluid and (b) we cannot infer the dominating era of a component of the universe by the evolution of the scale factor; i.e. Eq. (33) is not proper for the present discussion.

B. Remarks on the chaotic behavior

In the picture of the two coupled oscillators (Sec. II B) the dynamics indicated chaotic scattering, which would mean that the basins of attraction in the UDM box description should have a fractal structure. The basins of attraction are defined by the sink in which a trajectory ends up.

We start our analysis in the parameter range in which the five representative trajectories were chosen. Since all the five orbits start from $x = 0$, the transformation formula (32) gives that the plane on which they all lie is $X_{\partial U} = 0$. Figure 6 shows the basins of attraction on the latter plane; the positions of orbits 1 and 2 are indicated by the respective numbers. Actually, orbit 2 also indicates the area where 3, 4, and 5 approximately lie. The colors denoting the basins of each sink in Fig. 6 are smoothly separated with no evidence of smaller structures or mixing. Thus, there is no indication of fractal structure, which in turn implies absence of chaos. The absence of fractality was confirmed by choosing several different planes; a sample of
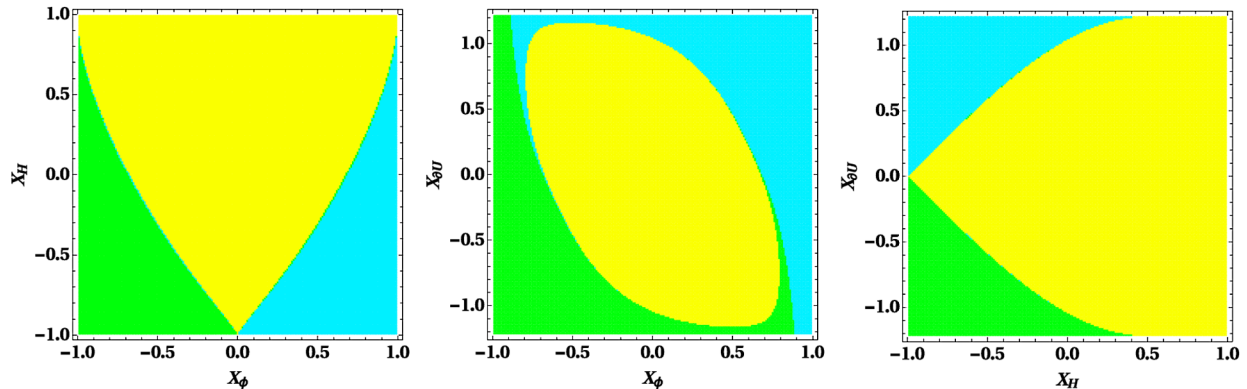

FIG. 7. The basins of attraction of the three sinks for the points in the planes $X_{\partial U} = 0$ (left panel), $X_H = 0$ (central panel) and $X_\phi = 0$ (right panel). The colors correspond to the basins of attraction of the three sinks indicated in Fig. 6.

them is shown in Fig. 7. This result is in agreement with the analysis of [16]. In particular, using the notation of [16], the condition for chaoticity is $\phi_0 > 4m_p/\sqrt{3}$: since $2\phi_0 = c^{-1}$ and $m_p^2 = 8\pi$ in our convention, our parameter c is not in the chaoticity range.

IV. CONCLUSIONS

We have analyzed a unified dark matter model in the background of a Friedmann-Robertson-Walker spacetime by both revisiting the study performed in [8] and providing new results. A specific variable transformation has allowed us to bound in a box the UDM model in the case of a FRW metric with positive spatial curvature. In this new set of variables the critical points of the dynamical system, i.e. sinks, sources and saddle points, were found and interpreted according to their dynamical and cosmological features. In particular, we have found that for the UDM models there are two dynamically distinct (but cosmologically indistinguishable) recollapsing scenarios, a feature that was not found in the previous study [8], and that at the vicinity of some of the saddle points the scalar field is behaving like a curvature fluid.

Characteristic evolution scenarios discussed in [8] were revisited and analyzed in the framework of the new variables. It was found that these scenarios start from a stiff matter equation of state $w = 1$, and most of them reach the de Sitter phase $w = -1$ by a smooth transition through all the values of w in between. At the de Sitter phase either the scenarios keep exponentially growing after a transient phase resembling a recollapse, or they actually recollapse. By taking advantage of the better insight provided by the new variables, we discussed the barotropic character of the UDM scalar field. While it makes sense to characterize *a critical point* by associating it to a constant effective EoS parameter w through Eq. (29), different w-dominated epochs *along an orbit* are not described by the respective scale factors given by Eq. (33) with constant EoS parameter: one has to keep in mind that the whole integrated effect along the orbit has to be considered; i.e. one has to employ Eq. (35).

Lastly, by studying the basins of the sinks in the variable space, we did not find any sign of fractal structure. This means that the system, for the range of parameters considered, is not chaotic, contrary to the findings of [8] but in agreement with the analysis of [16]. This contradiction might resemble the mixmaster case, where contradicting indications have resulted in a long debate on whether that system was chaotic or not; see e.g. [14,24] and references therein. However, as was mentioned in the introduction, Lyapunov-like indicators are not completely reliable tools for detecting chaos in unbounded systems.

So, given the current results and the investigation of [16], we can claim that the findings of [8] based on Lyapunov-like indicators were misleading.

APPENDIX: ALTERNATIVE FORM OF POTENTIAL

Let us consider here the case in which the potential is given by

$$U(\phi) = b_1 \left(1 + \cosh\left(\sqrt{\frac{3}{8}}\phi \right) \right)^3, \quad (A1)$$

where $b_1 \geq 0$ in order to have a non-negative mass for the scalar field. The dynamical system can be constructed in a completely analogous way as for the case of potential Eq. (4); the only difference being that in this case the variable $X_{\partial U}$ is bounded in the interval $[-(3/2)^{3/2}, (3/2)^{3/2}]$. This has repercussions on the location of some critical points of the system and their cosmological interpretation, but their total number and their stability character are unchanged with respect to the system analyzed in detail in the main text. For completeness, in Table II we list the critical points and their features. We can immediately see that the only cosmological difference regards the behavior of the model in the saddle points with coordinates $X_\phi = \pm 3/4$. By assuming the barotropic equation of state $w = 1/8$, the effective scale factor would be $a \sim t^{16/27}$, which is in between radiationlike and dustlike behavior.

TABLE II. Critical points of the system with potential given by Eq. (5), their stability and corresponding cosmological parameters.

$\{X_\phi, X_H, X_{\partial U}\}$	Stability	q	w
$\{0, -1, 0\}$	Source	-1	-1
$\{0, 1, 0\}$	Sink	-1	-1
$\{\pm 1, 1, \pm(\frac{3}{2})^{3/2}\}$	Source	2	1
$\{\pm 1, -1, \mp(\frac{3}{2})^{3/2}\}$	Sink	2	1
$\{\pm 1, 1, \mp(\frac{3}{2})^{3/2}\}$	Saddle	2	1
$\{\pm 1, -1, \pm(\frac{3}{2})^{3/2}\}$	Saddle	2	1
$\{\pm 3/4, 1, \pm(\frac{3}{2})^{3/2}\}$	Saddle	$\frac{11}{16}$	$1/8$
$\{\pm 3/4, -1, \mp(\frac{3}{2})^{3/2}\}$	Saddle	$\frac{11}{16}$	$1/8$
$\{\pm\frac{1}{\sqrt{3}}, \pm\frac{3\sqrt{3}}{4}, (\frac{3}{2})^{3/2}\}$	Saddle	0	$-1/3$
$\{\pm\frac{1}{\sqrt{3}}, \mp\frac{3\sqrt{3}}{4}, -(\frac{3}{2})^{3/2}\}$	Saddle	0	$-1/3$

[1] P. A. R. Ade *et al.*, Planck 2015 results. XIII. Cosmological parameters, Astron. Astrophys. **594,** A13 (2016).

[2] A. G. Riess, L. M. Macri, S. L. Hoffmann, D. Scolnic, S. Casertano, A. V. Filippenko, B. E. Tucker, M. J. Reid, D. O. Jones, J. M. Silverman, R. Chornock, P. Challis, W. Yuan, P. J. Brown, and R. J. Foley, A 2.4% determination of the local value of the Hubble constant, Astrophys. J. **826,** 56 (2016).

[3] M. Li, X.-D. Li, S. Wang, and Y. Wang, Dark energy: A brief review, Front. Phys. **8,** 828 (2013).

[4] C. Patrignani *et al.* (Particle Data Group Collaboration), Review of particle physics, Chin. Phys. C **40,** 100001 (2016).

[5] Y. Wu, S. Li, J. Lu, and X. Yang, The modified Chaplygin gas as a unified dark sector model, Mod. Phys. Lett. A **22,** 783 (2007).

[6] V. Sahni and L.-M. Wang, A new cosmological model of quintessence and dark matter, Phys. Rev. D **62,** 103517 (2000).

[7] D. Bertacca, S. Matarrese, and M. Pietroni, Unified dark matter in scalar field cosmologies, Mod. Phys. Lett. A **22,** 2893 (2007).

[8] G. Lukes-Gerakopoulos, S. Basilakos, and G. Contopoulos, Dynamics and chaos in the unified scalar field cosmology, Phys. Rev. D **77,** 043521 (2008).

[9] D. Bertacca, N. Bartolo, A. Diaferio, and S. Matarrese, How the scalar field of unified dark matter models can cluster, J. Cosmol. Astropart. Phys. 10 (2008) 023.

[10] S. Basilakos and G. Lukes-Gerakopoulos, Dynamics and constraints of the unified dark matter flat cosmologies, Phys. Rev. D **78,** 083509 (2008).

[11] D. Bertacca, N. Bartolo, and S. Matarrese, Unified dark matter scalar field models, Adv. Astron. **2010,** 904379 (2010).

[12] A. Paliathanasis, M. Tsamparlis, and S. Basilakos, Dynamical symmetries and observational constraints in scalar field cosmology, Phys. Rev. D **90,** 103524 (2014); A. Paliathanasis and M. Tsamparlis, Two scalar field cosmology: Conservation laws and exact solutions, Phys. Rev. D **90,** 043529 (2014).

[13] K. E. Starkov, On bounded and unbounded dynamics of the Hamiltonian system for unified scalar field cosmology, Phys. Lett. A **380,** 2064 (2016).

[14] G. Contopoulos, N. Voglis, and Ch. Efthymiopoulos, Chaos in relativity and cosmology, Celestial Mechanics and Dynamical Astronomy **73,** 1 (1999).

[15] D. N. Page, A fractal set of perpetually bouncing universe?, Classical Quantum Gravity **1,** 417 (1984).

[16] A. V. Toporensky, Regular and chaotic regimes in scalar field cosmology, SIGMA **2,** 037 (2006); A. Toporensky and P. Tretyakov, Certain aspects of regularity in scalar field cosmological dynamics, Reg. Chaotic Dyn. **12,** 357 (2007).

[17] O. Hrycyna and M. Szydlowski, Different faces of chaos in FRW models with scalar fields—geometrical point of view, Chaos Solitons Fractals **28,** 1252 (2006).

[18] M. S. Madsen and G. F. R. Ellis, The evolution of Ω in inflationary universes, Mon. Not. R. Astron. Soc. **234,** 67 (1988).

[19] M. Goliath and G. F. R. Ellis, Homogeneous cosmologies with a cosmological constant, Phys. Rev. D **60,** 023502 (1999).

[20] A. Campos and C. F. Sopuerta, Evolution of cosmological models in the brane-world scenario, Phys. Rev. D **63,** 104012 (2001).

[21] H. van Elst, C. Uggla, and J. Wainwright, Dynamical systems approach to G2 cosmology, Classical Quantum Gravity **19,** 51 (2002).

[22] M. Heinzle, N. Rohr, and C. Uggla, Matter and dynamics in closed cosmologies, Phys. Rev. D **71,** 083506 (2005).

[23] J. Kennedy and J. A. Yorke, Basins of Wada, Physica D (Amsterdam) **51D,** 213 (1991).

[24] N. J. Cornish and J. J. Levin, The Mixmaster Universe Is Chaotic, Phys. Rev. Lett. **78,** 998 (1997).

[25] Note that in the numerical analysis of Sec. III we choose a value of curvature which is marginally compatible with the observational bounds (as was done in [8]).

[26] P. J. Steinhardt, L. Wang, and I. Zlatev, Cosmological tracking solutions, Phys. Rev. D **59,** 123504 (1999).

[27] S. C. C. Ng, N. J. Nunes, and F. Rosati, Applications of scalar attractor solutions to cosmology, Phys. Rev. D **64,** 083510 (2001).

[28] An analogous condition on F would be relevant for the primordial inflationary era, as it determines the duration, or e-folds, of the exponential expansion.

[29] G. N. Remmen and S. M. Carroll, Attractor solutions in scalar-field cosmology, Phys. Rev. D **88,** 083518 (2013).

[30] J. Henrard, *The Adiabatic Invariant in Classical Mechanics,* Dynamics Reported Vol. 2 (Springer, New York, 1991).